Synthetic Protein-to-DNA Input Exchange for Protease Activity Detection Using CRISPR-Cas12a

Luca Capelli, [a‡] *Federica Pedrini,* [a‡] *Andrea C. Di Pede,* [b] *Neda Bagheri,* [b] *Simone Fortunati,* [a] *Marco Giannetto,* [a] *Monica Mattarozzi,* [a] *Roberto Corradini,* [a] *Alessandro Porchetta,* [b] *Alessandro Bertucci*[a]*

[a] *Department of Chemistry, Life Sciences and Environmental Sustainability, University of Parma, Parco Area Delle Scienze 17/A, 43124, Parma, Italy*

[b] *Department of Chemistry, University of Rome Tor Vergata, Via della Ricerca Scientifica 1, 00133 Rome, Italy*

KEYWORDS: CRISPR-Cas, protease, peptide nucleic acid, activity-based diagnostics, biosensors.

ABSTRACT

We present a novel activity-based detection strategy for matrix metalloproteinase 2 (MMP2), a critical cancer protease biomarker, leveraging a mechanism responsive to the proteolytic activity of MMP2 and its integration with CRISPR-Cas12a-assisted signal amplification. We designed a chemical translator comprising two functional units — a peptide and a peptide nucleic acid (PNA) — fused together. The peptide presents the substrate of MMP2, while the PNA serves as a nucleic acid output for subsequent processing. This chemical translator was immobilized on micrometric magnetic beads as a physical support for an activity-based assay. We incorporated into our design a single-stranded DNA partially hybridized with the PNA sequence and bearing a region complementary to the RNA guide of CRISPR-Cas12a. The target-induced nuclease activity of Cas12a results in the degradation

of FRET-labeled DNA reporters and amplified fluorescence signal, enabling detection of MMP2 in the low picomolar range, showing a limit of detection of 72 pg/mL. This study provides new design principles for a broader applicability of CRISPR-Cas-based biosensing.

Activity-based diagnostics are emerging sensing technologies that leverage the enzymatic activity of a protein to generate measurable outputs.[1] Unlike conventional immunoassays, these diagnostics offer unique advantages, including direct measurement of enzyme activity, specific substrate recognition, and real-time monitoring.[2,3] Beyond merely indicating the presence of a target protein, activity-based diagnostics can provide insights into its active biological state.[4] One specific area of interest for activity-based sensing is the detection and quantification of human proteases, a crucial class of hydrolytic enzymes responsible for degrading proteins, activating zymogens, and regulating numerous biological processes.[5–7] Among these, matrix metalloproteinases (MMPs), a family of zinc-dependent proteases capable of degrading extracellular matrix components, have garnered significant attention due to their potential as drug targets and biomarkers for cancer diagnosis.[8–10] In cancer, MMPs play a critical role in promoting invasion and metastasis, and their dysregulated expression profile serves as a distinctive trait of different tumours.[11–13] The activity-based quantification of specific MMPs can be achieved using fluorogenic peptide substrates. Typically, these peptides are labelled with a fluorophore/quencher pair, and a fluorescence signal is generated upon MMP-mediated hydrolytic cleavage.[14] Various classes of probes for this purpose are commercially available. However, these exhibit certain limitations, such as relatively high background signals and an inability to manipulate the output signal or integrate with signal amplification processes, which limits their sensitivity.[15,16] To address these challenges and enhance sensitivity, activity-based mechanisms have been combined with various optical and electrochemical assays, often leveraging nanomaterials to obtain amplification of the output signal.[17–23] Recently, innovative approaches involving nucleic acid-based amplification processes have emerged, which hold promise for advancing activity-based

protein detection through DNA nanotechnology.[24–26] One exceptionally powerful tool in nucleic acid diagnostics is signal amplification based on programmable single-stranded DNA (ssDNA) aspecific cleavage by preactivated CRISPR-Cas12a.[27–30] When the collateral cleavage of CRISPR-Cas12a is activated in the presence of FRET-labeled DNA reporters, a substantial signal amplification can be obtained, enabling ultrasensitive detection of the nucleic acid target.[31] To date, only a limited number of CRISPR-Cas-based sensing methods have been reported for the detection of targets such as proteins and small molecules, as this necessitates the development of non-trivial strategies for converting a non-nucleic acid target into a nucleic acid-based input for CRISPR-Cas activation.[27,32,33] The primary objective of our study was to explore a novel and straightforward avenue for integrating CRISPR-Cas12a amplification into a protease activity-based assay, thereby introducing a new modality for nucleic acid-based processing of protein inputs. We specifically focused on MMP2, a critical protease biomarker that has a fundamental role in various types of cancer, where its dysregulated expression is implicated in tumor advancement, invasion, metastasis, and angiogenesis.[34–37] To achieve the conversion of MMP2 enzymatic activity into a synthetic nucleic acid-based input for CRISPR-Cas12a, we designed a chemical translator that incorporates a peptide and a peptide nucleic acid (PNA) unit. The peptide unit presents the sequence specifically processed by MMP2, while the PNA unit facilitates the conversion of peptide cleavage into a nucleic acid output. This translator was anchored to magnetic microbeads (MBs), which serve as physical supports in the design of the activity-based assay. Hybridized with the PNA unit is a specific ssDNA sequence carrying a free region complementary to the CRISPR RNA (crRNA) of the CRISPR Cas12a system. This ssDNA serves as an activator of CRISPR-Cas12a. Upon MMP2 enzymatic cleavage, the nucleic acid portion (composed by a shortened peptide-PNA conjugate and by the DNA partially hybridized to it) is released, and the free DNA single strand segment can activate CRISPR-Cas12a, initiating the degradation of rationally designed hairpin DNA reporters labeled with a fluorophore/quencher pair. This process generates an amplified fluorescence signal enabling the quantification of MMP2 in the low picomolar range (Figure 1).

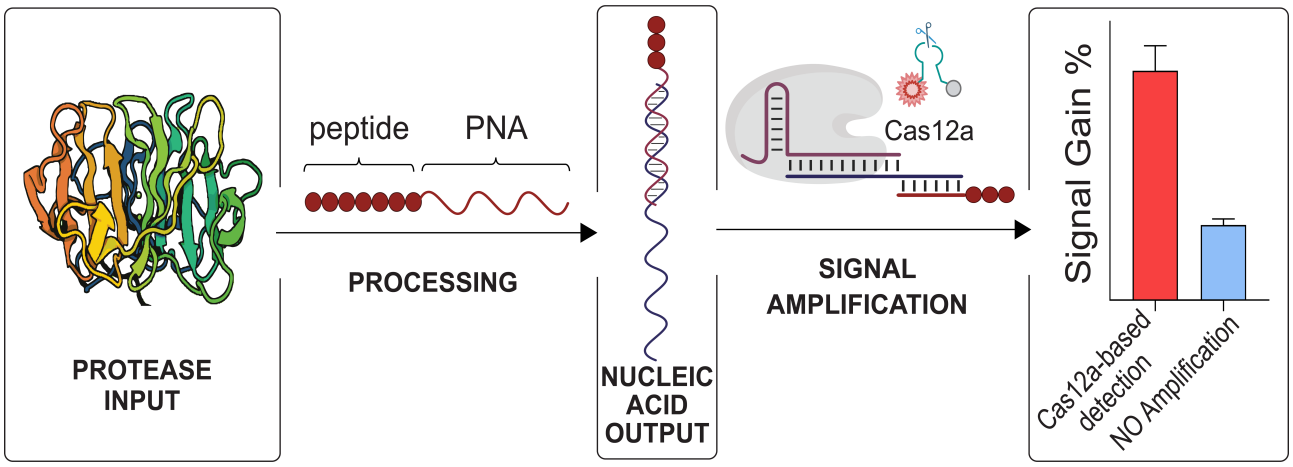

Figure 1. Schematic illustration of the proposed MMP2 activity-based detection method, leveraging a synthetic protein-to-DNA input exchange. A peptide-PNA chemical translator is used to convert MMP2 enzymatic activity into an input for CRISPR-Cas12a-based signal amplification.

We designed our chemical translator as a peptide-PNA conjugate where the peptide unit presents the specific substrate sequence of MMP2. We selected the sequence Gly-Pro-Leu-Gly-Val-Arg-Gly, which is reported to be specifically recognized by MMP2 and undergo hydrolytic cleavage of the peptide bond between the Gly-Val residues.[38] The PNA unit directly fused with the above peptide is a linear arbitrary 10-nt-long sequence (Figure 2a). Using a PNA sequence as the nucleic acid component of the translator enables specific economic and technological advantages. First, it is possible to synthesize the entire translator in a single round of solid phase synthesis harnessing conventional peptide chemistry, allowing for greatly reduced costs when compared to the synthesis/purchase of peptide-DNA hybrids. Second, given the exceptional stability of PNA:DNA duplexes[39,40], a relatively short PNA sequence can be used as an anchor for hybridization with the CRISPR-Cas12a target ssDNA. This facilitates synthesis and minimizes the length of the duplex region in the fragment of the translator serving as the new input for CRISPR-Cas12a (Figure 1), therefore limiting possible steric hindrance effects. In addition, we included an azide group on the 5'-end of the translator to enable click chemistry for the immobilization of the probe on a solid support

(Figure 2a). The peptide-PNA translator was synthesized using conventional FMOC-based solid phase chemistry, purified via HPLC and its identity confirmed using mass spectrometry (see Supporting Information, Material and Methods, and Figure S1, S2). To validate the functionality of our synthetic probe as a substrate for MMP2, we demonstrated hydrolysis of the peptide unit at the anticipated cleavage site. After incubating the translator and the protease together, we analyzed the reaction products by means of HPLC-ESI-HRMS (Figure 2b, c). As shown in Figure 2c, one peak in the chromatogram corresponded to the unreacted translator, which was used in large excess in this experiment, and the other two main peaks could be associated to the two expected fragments generating from hydrolytic cleavage of the peptide unit, thus confirming that the peptide-PNA translator can effectively serve as a synthetic substrate for MMP2 (Figure 2c).

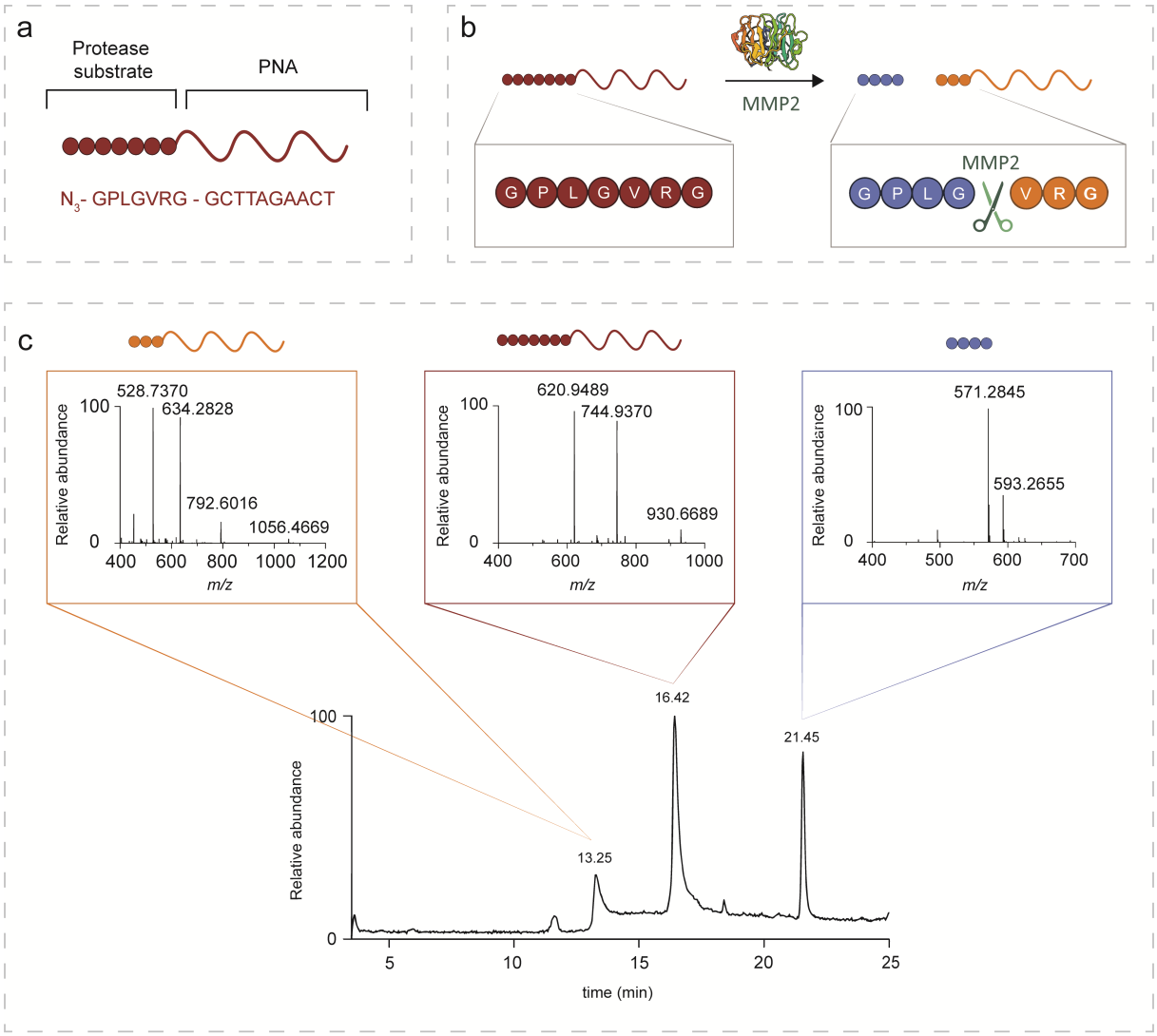

Figure 2. Design of the peptide-PNA chemical translator and HPLC-HRMS analysis of protease cleavage products. (a) Illustration of the molecular design of the chemical translator, reporting the aminoacidic sequence of the peptide unit and the nucleobase sequence of the PNA unit. An azide group is conjugated to the 5'-end of the probe to enable click chemistry for anchoring to solid supports. A fluorescent version of the translator was obtained by conjugating 5(6)-Carboxy-tetramethylrhodamine (TAMRA) to additional lysine residue present at the 3'-end. (b) Schematic representation of the MMP2-mediated enzymatic cleavage of the chemical translator (red circle-line probe), highlighting the cleavage site and the formation of two reaction products, a small peptide fragment (blue circles) and a larger fragment containing the PNA unit (orange circles + orange line). (c) HPLC-ESI-HRMS chromatogram of the chemical translator after incubation with MMP2 (24 h, 37 °C, [MMP2]:[translator] 1:10). The three main peaks correspond to the to the PNA-containing fragment (rt 13.25 min, *m/z* = 528.7370 $[M+6H]^{6+}$, 634.2828 $[M+5H]^{5+}$, 792.6016 $[M+4H]^{4+}$, 1056.4669 $[M+3H]^{3+}$ orange box), to unreacted molecular translator present in large excess in the reaction mixture (rt 16.42 min, *m/z* = 620.9489 $[M+6H]^{6+}$, 744.9370 $[M+5H]^{5+}$, 930.6689 $[M+4H]^{4+}$ red box), and to the peptide fragment (rt 21.45 min, m/z = 571.2845 $[M+H]^{+}$, 593.2655 $[M+Na]^{+}$ blue box).

We resorted to magnetic beads as solid platforms for physical anchoring of the chemical translator. This enables the isolation of the cleaved PNA-containing fragment, serving as a nucleic acid-based input for further signal elaboration. We employed micrometer-sized magnetic beads functionalized with amine groups on their surfaces. We chose to covalently immobilize the translator onto the beads through a copper-free strain-promoted alkyne-azide cycloaddition (SPAAC) reaction, which has the advantage of being orthogonal to all the other reactive groups in the peptide-PNA sequence. To do so, we first transformed the amine groups on the bead surface into SPAAC-reactive cyclooctyne groups by reacting them with dibenzocyclooctyne-N-hydroxysuccunimidyl ester (DBCO-NHS) (Fig. 3a). Zeta potential measurements of the changes in the net surface charge of the magnetic beads after

treatment with different concentrations of DBCO-NHS were used to study and optimize the functionalization reaction (Figure S3). We then explored the most advantageous conditions for the SPAAC reaction by evaluating different solvents.[41] To validate the presence of the translator on the magnetic bead surface, we used a version of the translator labeled with tetramethylrhodamine (TAMRA). This allowed us to calculate the quantity of translator immobilized on the beads by means of fluorescence spectroscopy (Figure S4, Table S1). Conducting the SPAAC reaction in TRIS buffer enabled the construction of a loading curve for standardizing the surface probe density, showing that a solution of 10 μM of peptide-PNA conjugate was required to maximize the efficiency of the functionalization process, affording 7.68 nmoles of translator attached per mg of magnetic beads (Figure S4). Characterization of the different functionalization steps was performed by means of zeta potential measurements, ATR-FT-IR spectroscopy, and two-photon fluorescence microscopy (Fig. 3b, Figure S6, S7).

Next, we demonstrated that MMP2 could effectively hydrolyze the peptide-PNA translator anchored on the magnetic bead surface. To this end, we functionalized the magnetic beads with a fluorescent TAMRA-labeled version of the translator (see SI). After incubation with MMP2 and magnetic separation of the beads, it was possible to detect and quantify the TAMRA-labeled PNA-containing cleavage product in the supernatant by using fluorescence spectroscopy (Fig. 3c). Based on the fluorescence emission intensity of the supernatant, the cleavage process effectively occurred in 2 hours, which aligns with what is reported for other activity-based sensing platforms for MMP2 (Fig. 3d).[42] We also evaluated the specificity of our sensing platform for MMP2 when exposed to other proteases from the MMP family, namely MMP1, MMP9, and MMP12. As reported in the literature, some level of cross-reactivity could be observed in this case.[43] Fluorescence spectroscopy measurements of the supernatant after physical separation of the translator-modified beads showed that the sensing platform exhibited a substantial specificity for MMP2 (Fig. 3e). Quantitative analysis of the concentration of the TAMRA-labeled PNA-containing cleavage product in the supernatant after incubation of the functionalized magnetic beads (1 mg/mL, equivalent to 10 μM of translator in 150

µL of assay volume) with varying concentrations of MMP2 allowed us to estimate a limit of detection (LOD) of 104 pM for the current non-amplified sensing platform (Fig. 3f).

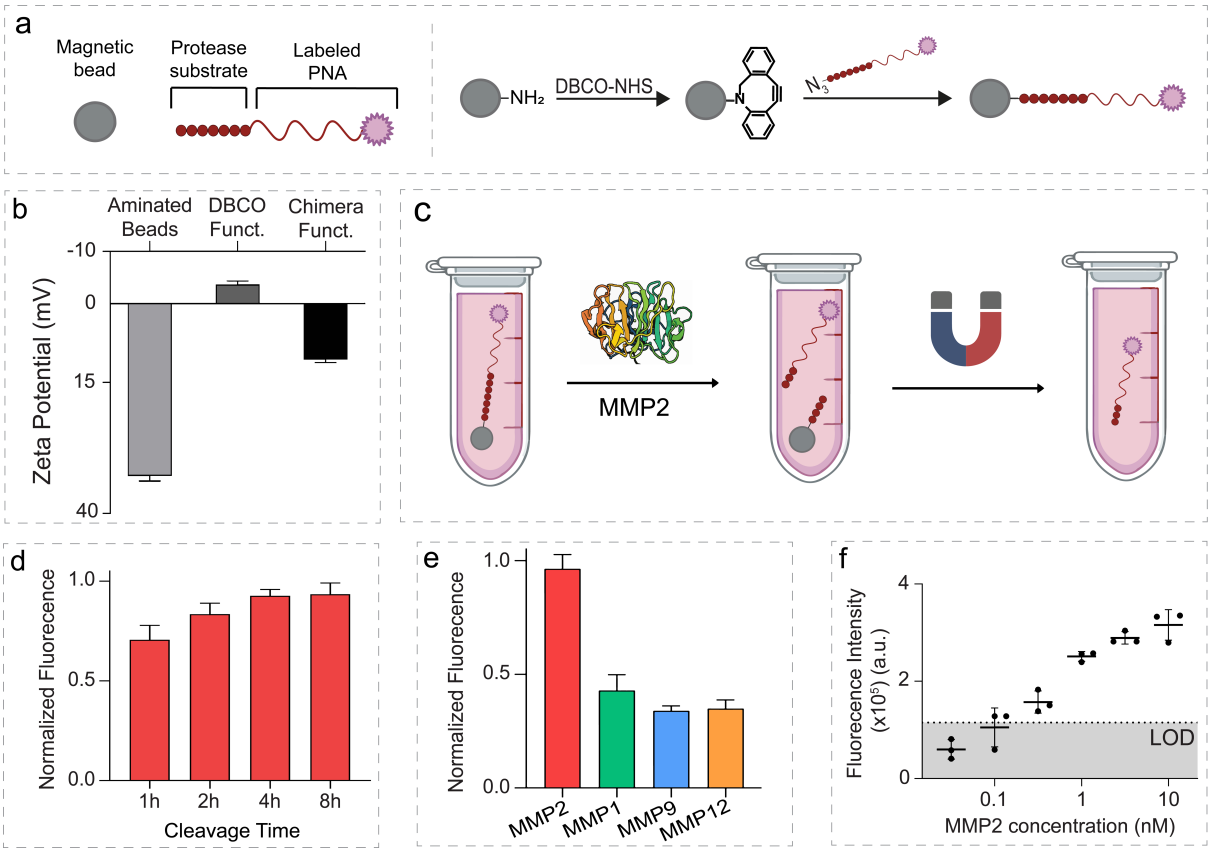

Figure 3. Design of the sensing platform and characterization of the activity-based sensing mechanism. (a) Multistep functionalization scheme of the magnetic beads with the chemical translator. Bifunctional DBCO-NHS allows for converting the amine groups initially present on the bead surface into DBCO functionalities. The peptide-PNA translator was then grafted onto these beads through a SPAAC reaction between the azide moiety on the 5'-end of the peptide unit of the translator and DBCO. (b) Zeta potential mesurements during the various functionalization steps. After functionalization with DBCO, the zeta potential of a dispersion of the magnetic beads in PBS buffer shifts from 33 ± 1 mV to - 4 ± 1 mV. Conjugation with the chemical translator increases the zeta potential to 11 ± 1 mV (n = 3, mean + SD). (c) Illustration of the MMP2 cleavage assay using magnetic beads functionalized with a fluorophore-tagged chemical translator. When the sensing platform is incubated with MMP2, proteolytic cleavage followed by magnetic separation of the beads

results in a supernatant enriched in the PNA-containing cleavage product. (d) Normalized fluorescence intensity obtained for the cleavage assay conducted using different MMP2 incubation times ([MMP2] 100 nM, magnetic beads 1mg/mL, n = 3, mean + SD). (e) Normalized fluorescence intensity obtained with MMP2 (100 nM) and other non-specific MMPs (100 nM) (n = 3, mean + SD). (f) Fluorescence intensity values obtained for the assay conducted using different concentrations of MMP2 in the range of 0.03 - 10 nM, from which it was possible to calculate a LOD of 104 pM (n = 3, mean ± SD), calculated as the concentration of MMP2 leading to a signal change equal to 3 times the intensity of the background (absence of the target).

Next, to achieve translation of MMP2 enzymatic activity into a DNA-based input for the activation of CRISPR-Cas12a, we integrated a strategy for protein-to-DNA input exchange into the above sensing platform. Signal amplification based on the use of CRISPR-Cas12a leverages the target-induced indiscriminate nuclease activity (trans-cleavage) of Cas12a, which can be used for degrading nearby single-stranded DNA reporter labeled with a fluorophore/quencher pair.[31,44,45] CRISPR-Cas12a can recognize either complementary single-stranded (ss) or double-stranded (ds) DNA sequences.[46] We designed a ssDNA sequence encompassing both a domain complementary to the sequence of the PNA unit in the translator and a second domain serving as the target sequence for the crRNA complexed with Cas12a (Figure 4a and SI). By preforming the PNA:DNA heteroduplex on the magnetic bead surface, the sensing platform could release the DNA-containing fragment in the supernatant following MMP2-mediated cleavage of the translator (Fig. 4a). The hybridization between the crRNA in the CRISPR-Cas12a complex and its target ssDNA in the supernatant activates the trans-endonuclease activity of Cas12a, allowing to generate an amplified fluorescence signal through the indiscriminate degradation of hairpin DNA reporters labeled with a FAM/BHQ fluorophore/quencher pair. We chose to employ hairpin DNA reporters based on a recent publication demonstrating that such conformation enables enhanced sensitivity compared to conventional linear DNA reporters.[31] Figure 4b reports representative kinetic fluorescence measurements of MMP2-

dependent Cas12a-mediated degradation of the hairpin reporters, showing that the amplification process proceeds to completion in less than 2 hours. The endpoint fluorescence intensity values were used to build a calibration curve that showed linearity in the Log MMP2 concentration range 1 – 100 pM, with a LOD of 1 pM, corresponding to 72 pg/mL MMP2 (Fig. 4c). This LOD is orders of magnitude lower than average commercially available peptide-based kits.[47] Figure 4d reports signal gain % values calculated for different concentrations of MMP2 after CRISPR-Cas12a-based processing of the MMP2-derived nucleic acid output. The resulting signal amplification leads to a significant increase in the signal gain % values with respect to those that can be calculated from the non-amplified fluorescence intensity values reported in Figure 3c.

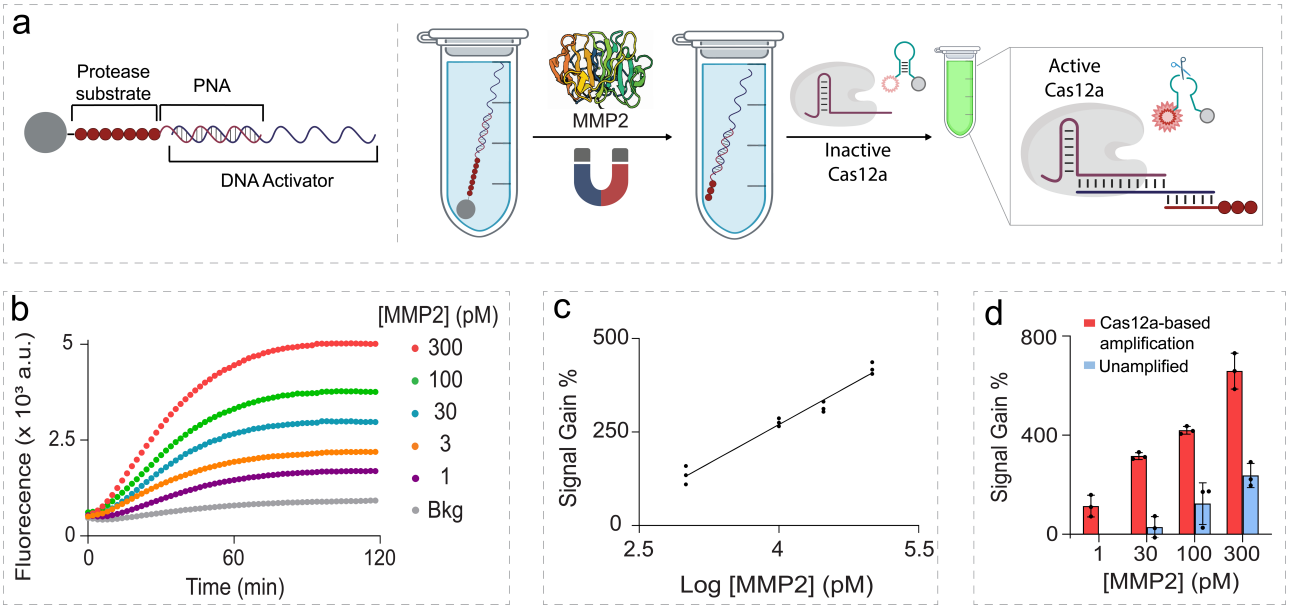

Figure 4. CRISPR-Cas12a-based amplification of MMP2-derived nucleic acid output. (a) A pictorial illustration of the proposed MMP2 acivity-based assay using CRISPR-Cas12a-based signal amplification. The peptide-PNA translator on the magnetic bead surface is hybridized with a ssDNA sequence serving as the trigger input for target-induced CRISPR-Cas12 trans-cleavage nuclease activity. Following incubation with MMP2 and magnetic separation of the beads, the nucleic acid-containing cleavage product enriches the supernatant. This is incubated with a preformed crRNA/Cas12a complex (20 nM) in the presence of an excess of ssDNA hairpin reporter (100 nM).

(b) Fluorescence kinetic profiles of CRISPR-Cas12a trans-cleavage activity (i.e., Cas12a-mediated degradation of the DNA hairpin reporters) upon interaction with MMP2-derived ssDNA activator in the MMP2 concentration range 1 - 300 pM. (c) Calibration curve obtained through a linear fit of signal gain % values in the 1 - 100 pM MMP2 concentration range. The curve is described by the following equation $y = (-281.3 \pm 32.9) + (137.9 \pm 7.9)\ x$, $R^2 = 0.97$ (d) Signal gain % values, calculated at the 2-hour endpoint, obtained for CRISPR-Cas12a-based (red bars) and unamplified fluorescence assays (blue bars) for different concentrations of MMP2 (n = 3, mean ± SD).

In conclusion, we successfully developed a novel sensing platform for the activity-based detection of MMP2, enabled by a protein-to-DNA input exchange mechanism combined with CRISPR-Cas12a signal amplification. Our CRISPR-Cas12a-assisted sensing platform demonstrated remarkable sensitivity and an LOD as low as 72 pg/mL MMP2, outperforming commercially available activity-based fluorogenic kits. The present LOD is also particularly relevant as it falls within the early detection range, which is considered to be at least below 5 ng/mL for this type of protein target.[48] Key in our design is the use of a chimeric peptide-PNA conjugate, serving as a molecular translator for the conversion of an enzyme-based input into a nucleic acid-based output. The nature of the translator allows for adaption to the detection of other specific MMPs and enzymes simply by modifying the peptide substrate sequence, making the presented strategy a highly versatile platform technology for the realization of CRISPR-Cas-based detection of protein targets. The presented strategy also showcases a new application space for CRISPR-Cas-based biosensing, highlighting its potential beyond nucleic acid diagnostics.[49,50] As this approach enables the generation of a protein-derived arbitrary nucleic acid-based input, many other amplification techniques, such as those based on CRISPR-Cas13, hybridization chain reaction or polymerase chain reaction, could be explored, also opening the possibility to perform multiplexing biomarker analysis. From a different angle, this work also demonstrates a new possible modality for enzyme-controlled DNA-based computation, enabling the integration of proteolytic activity with DNA nanotechnology.[26,51–54]

ASSOCIATED CONTENT

Supporting Information

Materials and methods, including nucleic acid sequences, a description of the synthesis of the peptide-PNA conjugate and of the multistep functionalization of magnetic beads, and a protocol for the CRISPR-Cas12a assay; supplementary figures reporting FT-IR spectra, fluorescence emission spectra, zeta potential measurements, a chromatogram for the peptide-PNA conjugate characterization, and a two-photon microscopy image of functionalized magnetic beads.

AUTHOR INFORMATION

Corresponding Author

Alessandro Bertucci - *Department of Chemistry, Life Sciences and Environmental Sustainability, University of Parma, 43124, Parma, Italy.*
ORCID: 0000-0003-4842-9909.
Email: alessandro.bertucci@unipr.it

Authors

Luca Capelli - *Department of Chemistry, Life Sciences and Environmental Sustainability, University of Parma, 43124, Parma, Italy.*

Federica Pedrini - *Department of Chemistry, Life Sciences and Environmental Sustainability, University of Parma, 43124, Parma, Italy.*

Andrea C. Di Pede - *Department of Chemistry, University of Rome Tor Vergata, Via della Ricerca Scientifica 1, 00133 Rome, Italy.*

Neda Bagheri - *Department of Chemistry, University of Rome Tor Vergata, Via della Ricerca Scientifica 1, 00133 Rome, Italy.*

Simone Fortunati - *Department of Chemistry, Life Sciences and Environmental Sustainability, University of Parma, 43124, Parma, Italy.*

Marco Giannetto - *Department of Chemistry, Life Sciences and Environmental Sustainability, University of Parma, 43124, Parma, Italy.*

Monica Mattarozzi - *Department of Chemistry, Life Sciences and Environmental Sustainability, University of Parma, 43124, Parma, Italy.*

Roberto Corradini - *Department of Chemistry, Life Sciences and Environmental Sustainability, University of Parma, 43124, Parma, Italy.*

Alessandro Porchetta - *Department of Chemistry, University of Rome Tor Vergata, Via della Ricerca Scientifica 1, 00133 Rome, Italy.*

Author Contributions

‡L.C. and F.P. contributed equally. The manuscript was written through contributions of all authors. All authors have given approval to the final version of the manuscript.

Notes

The authors declare no competing financial interest.

ACKNOWLEDGMENTS

This research was granted by University of Parma through the action Bando di Ateneo 2022 per la ricerca co-funded by MUR-Italian Ministry of Universities and Research - D.M. 737/2021 - PNR - PNRR – NextGenerationEU. This work was supported by the Guido Berlucchi Foundation Mini Grant codice progetto BERTUCCI_2022_FONDBERLUCCHI. A.B. and A.P. acknowledge funding from the Italian Ministry of University and Research (Project of National Interest, PRIN, 2022FPYZ2N). This work has benefited from the equipment and framework of the COMP-HUB and COMP-R Initiatives, funded by the 'Departments of Excellence' program of the Italian Ministry for University and Research (MIUR, 2018-2022 and MUR, 2023-2027).

REFERENCES

(1) Soleimany, A. P.; Bhatia, S. N. Activity-Based Diagnostics: An Emerging Paradigm for Disease Detection and Monitoring. *Trends. Mol. Med.* **2020**, *26* (5), 450–468. https://doi.org/10.1016/j.molmed.2020.01.013.

(2) Muir, R. K.; Guerra, M.; Bogyo, M. M. Activity-Based Diagnostics: Recent Advances in the Development of Probes for Use with Diverse Detection Modalities. *ACS Chem. Biol.* **2022**, *17* (2), 281–291. https://doi.org/10.1021/acschembio.1c00753.

(3) Kandell, R. M.; Kudryashev, J. A.; Kwon, E. J. Targeting the Extracellular Matrix in Traumatic Brain Injury Increases Signal Generation from an Activity-Based Nanosensor. *ACS Nano* **2021**, *15* (12), 20504–20516. https://doi.org/10.1021/acsnano.1c09064.

(4) Kudryashev, J. A.; Madias, M. I.; Kandell, R. M.; Lin, Q. X.; Kwon, E. J. An Activity-Based Nanosensor for Minimally-Invasive Measurement of Protease Activity in Traumatic Brain Injury. *Adv. Funct. Mater.* **2023**, *33* (28). https://doi.org/10.1002/adfm.202300218.

(5) Nagano, N.; Ichihashi, Y.; Komatsu, T.; Matsuzaki, H.; Hata, K.; Watanabe, T.; Misawa, Y.; Suzuki, M.; Sakamoto, S.; Kagami, Y.; Kashiro, A.; Takeuchi, K.; Kanemitsu, Y.; Ochiai, H.; Watanabe, R.; Honda, K.; Urano, Y. Development of Fluorogenic Substrates for Colorectal Tumor-Related Neuropeptidases for Activity-Based Diagnosis. *Chem. Sci.* **2023**, *14* (17), 4495–4499. https://doi.org/10.1039/d2sc07029d.

(6) Sanman, L. E.; Bogyo, M. Activity-Based Profiling of Proteases. *Annu. Rev. Biochem.* **2014**, *83*, 249–273. https://doi.org/10.1146/annurev-biochem-060713-035352.

(7) Zmudzinski, M.; Malon, O.; Poręba, M.; Drąg, M. Imaging of Proteases Using Activity-Based Probes. *Curr. Opin. Chem. Biol.* **2023**, *74*. https://doi.org/10.1016/j.cbpa.2023.102299.

(8) Zhang, H.; Wu, M.; Ta, H. T.; Xu, Z. P.; Zhang, R. Recent Development and Applications of Sensors for the Detection of Matrix Metalloproteinases. *Adv. Mater. Technol.* **2023**, *8*. https://doi.org/10.1002/admt.202201786.

(9) Ćwilichowska, N.; Świderska, K. W.; Dobrzyń, A.; Drąg, M.; Poręba, M. Diagnostic and Therapeutic Potential of Protease Inhibition. *Mol. Aspects Med.* **2022**, *88*. https://doi.org/10.1016/j.mam.2022.101144.

(10) Dudani, J. S.; Warren, A. D.; Bhatia, S. N. Harnessing Protease Activity to Improve Cancer Care. *Annu. Rev. Cancer Biol.* **2017**, *2*, 353–376. https://doi.org/10.1146/annurev-cancerbio.

(11) Egeblad, M.; Werb, Z. New Functions for the Matrix Metalloproteinases in Cancer Progression. *Nat. Rev. Cancer* **2002**, *2* (3), 161–174. https://doi.org/10.1038/nrc745.

(12) Quintero-Fabián, S.; Arreola, R.; Becerril-Villanueva, E.; Torres-Romero, J. C.; Arana-Argáez, V.; Lara-Riegos, J.; Ramírez-Camacho, M. A.; Alvarez-Sánchez, M. E. Role of Matrix Metalloproteinases in Angiogenesis and Cancer. *Front. Oncol.* **2019**, *9*. https://doi.org/10.3389/fonc.2019.01370.

(13) Gobin, E.; Bagwell, K.; Wagner, J.; Mysona, D.; Sandirasegarane, S.; Smith, N.; Bai, S.; Sharma, A.; Schleifer, R.; She, J. X. A Pan-Cancer Perspective of Matrix Metalloproteases (MMP) Gene Expression Profile and Their Diagnostic/Prognostic Potential. *BMC Cancer* **2019**, *19* (1). https://doi.org/10.1186/s12885-019-5768-0.

(14) Fields, G. B. Using Fluorogenic Peptide Substrates to Assay Matrix Metalloproteinases. In *Matrix Metalloproteinase Protocols*; Clark, I. M., Young, D. A., Rowan, A. D., Eds.; Humana Press , 2010; Vol. 622, pp 393–433. https://doi.org/10.1007/978-1-60327-299-5_24.

(15) Pham, W.; Choi, Y.; Weissleder, R.; Tung, C. H. Developing a Peptide-Based near-Infrared Molecular Probe for Protease Sensing. *Bioconjug. Chem.* **2004**, *15* (6), 1403–1407. https://doi.org/10.1021/bc049924s.

(16) Ryu, J. H.; Lee, A.; Lee, S.; Ahn, C. H.; Park, J. W.; Leary, J. F.; Park, S.; Kim, K.; Kwon, I. C.; Youn, I. C.; Choi, K. "One-Step" Detection of Matrix Metalloproteinase Activity Using a Fluorogenic Peptide

Probe-Immobilized Diagnostic Kit. *Bioconjug. Chem.* **2010**, *21* (7), 1378–1384. https://doi.org/10.1021/bc100008b.

(17) Li, X.; Deng, D.; Xue, J.; Qu, L.; Achilefu, S.; Gu, Y. Quantum Dots Based Molecular Beacons for in Vitro and in Vivo Detection of MMP-2 on Tumor. *Biosens. Bioelectron.* **2014**, *61*, 512–518. https://doi.org/10.1016/j.bios.2014.05.035.

(18) Feng, D.; Zhang, Y.; Feng, T.; Shi, W.; Li, X.; Ma, H. A Graphene Oxide-Peptide Fluorescence Sensor Tailor-Made for Simple and Sensitive Detection of Matrix Metalloproteinase 2. *Chem. Commun.* **2011**, *47* (38), 10680–10682. https://doi.org/10.1039/c1cc13975d.

(19) Welser, K.; Adsley, R.; Moore, B. M.; Chan, W. C.; Aylott, J. W. Protease Sensing with Nanoparticle Based Platforms. *Analyst* **2011**, *136* (1), 29–41. https://doi.org/10.1039/c0an00429d.

(20) Jin, Z.; Dridi, N.; Palui, G.; Palomo, V.; Jokerst, J. V.; Dawson, P. E.; Sang, Q. X. A.; Mattoussi, H. Quantum Dot-Peptide Conjugates as Energy Transfer Probes for Sensing the Proteolytic Activity of Matrix Metalloproteinase-14. *Anal. Chem.* **2023**, *95* (5), 2713–2722. https://doi.org/10.1021/acs.analchem.2c03400.

(21) Lei, Z.; Zhang, H.; Wang, Y.; Meng, X.; Wang, Z. Peptide Microarray-Based Metal Enhanced Fluorescence Assay for Multiple Profiling of Matrix Metalloproteinases Activities. *Anal. Chem.* **2017**, *89* (12), 6749–6757. https://doi.org/10.1021/acs.analchem.7b01037.

(22) Biela, A.; Watkinson, M.; Meier, U. C.; Baker, D.; Giovannoni, G.; Becer, C. R.; Krause, S. Disposable MMP-9 Sensor Based on the Degradation of Peptide Cross-Linked Hydrogel Films Using Electrochemical Impedance Spectroscopy. *Biosens. Bioelectron.* **2015**, *68*, 660–667. https://doi.org/10.1016/j.bios.2015.01.060.

(23) Kou, B. B.; Chai, Y. Q.; Yuan, Y. L.; Yuan, R. PtNPs as Scaffolds to Regulate Interenzyme Distance for Construction of Efficient Enzyme Cascade Amplification for Ultrasensitive Electrochemical Detection of MMP-2. *Anal. Chem.* **2017**, *89* (17), 9383–9387. https://doi.org/10.1021/acs.analchem.7b02210.

(24) Li, Y.; Liu, W.; Xu, Q.; Hu, J.; Zhang, C. yang. Construction of a Sensitive Protease Sensor with DNA-Peptide Conjugates for Single-Molecule Detection of Multiple Matrix Metalloproteinases. *Biosens. Bioelectron.* **2020**, *169*. https://doi.org/10.1016/j.bios.2020.112647.

(25) Luo, X.; Zhao, J.; Xie, X.; Liu, F.; Zeng, P.; Lei, C.; Nie, Z. Proteolysis-Responsive Rolling Circle Transcription Assay Enabling Femtomolar Sensitivity Detection of a Target Protease Biomarker. *Anal. Chem.* **2020**, *92* (24), 16314–16321. https://doi.org/10.1021/acs.analchem.0c04427.

(26) Bui, H.; Brown, C. W.; Buckhout-White, S.; Díaz, S. A.; Stewart, M. H.; Susumu, K.; Oh, E.; Ancona, M. G.; Goldman, E. R.; Medintz, I. L. Transducing Protease Activity into DNA Output for Developing Smart Bionanosensors. *Small* **2019**, *15* (14). https://doi.org/10.1002/smll.201805384.

(27) Kaminski, M. M.; Abudayyeh, O. O.; Gootenberg, J. S.; Zhang, F.; Collins, J. J. CRISPR-Based Diagnostics. *Nat. Biomed. Eng.* **2021**, *5* (7), 643–656. https://doi.org/10.1038/s41551-021-00760-7.

(28) Li, S. Y.; Cheng, Q. X.; Li, X. Y.; Zhang, Z. L.; Gao, S.; Cao, R. B.; Zhao, G. P.; Wang, J.; Wang, J. M. CRISPR-Cas12a-Assisted Nucleic Acid Detection. *Cell Discov.* **2018**, *4* (1). https://doi.org/10.1038/s41421-018-0028-z.

(29) Chen, J. S.; Ma, E.; Harrington, L. B.; Da Costa, M.; Tian, X.; Palefsky, J. M.; Doudna, J. A. CRISPR-Cas12a Target Binding Unleashes Indiscriminate Single-Stranded DNase Activity. *Science* **2018**, *360*, 436–439.

(30) Broughton, J. P.; Deng, X.; Yu, G.; Fasching, C. L.; Servellita, V.; Singh, J.; Miao, X.; Streithorst, J. A.; Granados, A.; Sotomayor-Gonzalez, A.; Zorn, K.; Gopez, A.; Hsu, E.; Gu, W.; Miller, S.; Pan, C. Y.;

Guevara, H.; Wadford, D. A.; Chen, J. S.; Chiu, C. Y. CRISPR–Cas12-Based Detection of SARS-CoV-2. *Nat. Biotechnol.* **2020**, *38* (7), 870–874. https://doi.org/10.1038/s41587-020-0513-4.

(31) Rossetti, M.; Merlo, R.; Bagheri, N.; Moscone, D.; Valenti, A.; Saha, A.; Arantes, P. R.; Ippodrino, R.; Ricci, F.; Treglia, I.; Delibato, E.; Van Der Oost, J.; Palermo, G.; Perugino, G.; Porchetta, A. Enhancement of CRISPR/Cas12a Trans-Cleavage Activity Using Hairpin DNA Reporters. *Nucleic Acids Res.* **2022**, *50* (14), 8377–8391. https://doi.org/10.1093/nar/gkac578.

(32) Li, J.; Yang, S.; Zuo, C.; Dai, L.; Guo, Y.; Xie, G. Applying CRISPR-Cas12a as a Signal Amplifier to Construct Biosensors for Non-DNA Targets in Ultralow Concentrations. *ACS Sens.* **2020**, *5* (4), 970–977. https://doi.org/10.1021/acssensors.9b02305.

(33) Xiong, Y.; Zhang, J.; Yang, Z.; Mou, Q.; Ma, Y.; Xiong, Y.; Lu, Y. Functional DNA Regulated CRISPR-Cas12a Sensors for Point-of-Care Diagnostics of Non-Nucleic-Acid Targets. *J. Am. Chem. Soc.* **2020**, *142* (1), 207–213. https://doi.org/10.1021/jacs.9b09211.

(34) Dutta, A.; Li, J.; Lu, H.; Akech, J.; Pratap, J.; Wang, T.; Zerlanko, B. J.; Gerald, T. J. F.; Jiang, Z.; Birbe, R.; Wixted, J.; Violette, S. M.; Stein, J. L.; Stein, G. S.; Lian, J. B.; Languino, L. R. Integrin Avb6 Promotes an Osteolytic Program in Cancer Cells by Upregulating MMP2. *Cancer Res.* **2014**, *74* (5), 1598–1608. https://doi.org/10.1158/0008-5472.CAN-13-1796.

(35) Tuszynski, G.; Jhon, A. The Role of Matrix Metalloproteinases in Tumor Angiogenesis and Tumor Metastasis. *Pathol. Oncol. Res.* **2001**, *7*, 14–23.

(36) Xie, T. X.; Wei, D.; Liu, M.; Gao, A. C.; Ali-Osman, F.; Sawaya, R.; Huang, S. Stat3 Activation Regulates the Expression of Matrix Metalloproteinase-2 and Tumor Invasion and Metastasis. *Oncogene* **2004**, *23* (20), 3550–3560. https://doi.org/10.1038/sj.onc.1207383.

(37) Jezierska, A.; Motyl, T. Matrix Metalloproteinase-2 Involvement in Breast Cancer Progression: A Mini-Review. *Med. Sci. Monit.* **2009**, *15* (2), RA32–RA40.

(38) Von Maltzahn, G.; Harris, T. J.; Park, J. H.; Min, D. H.; Schmidt, A. J.; Sailor, M. J.; Bhatia, S. N. Nanoparticle Self-Assembly Gated by Logical Proteolytic Triggers. *J. Am. Chem. Soc.* **2007**, *129* (19), 6064–6065. https://doi.org/10.1021/ja0704611.

(39) Jensen, K. K.; Ørum, H.; Nielsen, P. E.; Nordén, B. Kinetics for Hybridization of Peptide Nucleic Acids (PNA) with DNA and RNA Studied with the BIAcore Technique. *Biochemistry* **1997**, *36* (16), 5072–5077. https://doi.org/10.1021/bi9627525.

(40) Egholm, M.; Buchardt, O.; Christensen, L.; Behrens, C.; Freier, S. M.; Driver, D. A.; Berg, R. H.; Kim, S. K.; Norden, B.; Nielsen, P. E. PNA Hybridizes to Complementary Oligonucleotides Obeying the Watson–Crick Hydrogen-Bonding Rules. *Nature* **1993**, *365* (6446), 566–568. https://doi.org/10.1038/365566a0.

(41) Davis, D. L.; Price, E. K.; Aderibigbe, S. O.; Larkin, M. X. H.; Barlow, E. D.; Chen, R.; Ford, L. C.; Gray, Z. T.; Gren, S. H.; Jin, Y.; Keddington, K. S.; Kent, A. D.; Kim, D.; Lewis, A.; Marrouche, R. S.; O'Dair, M. K.; Powell, D. R.; Scadden, M. H. C.; Session, C. B.; Tao, J.; Trieu, J.; Whiteford, K. N.; Yuan, Z.; Yun, G.; Zhu, J.; Heemstra, J. M. Effect of Buffer Conditions and Organic Cosolvents on the Rate of Strain-Promoted Azide-Alkyne Cycloaddition. *J. Org. Chem.* **2016**, *81* (15), 6816–6819. https://doi.org/10.1021/acs.joc.6b01112.

(42) Liu, L.; Chu, H.; Yang, J.; Sun, Y.; Ma, P.; Song, D. Construction of a Magnetic-Fluorescent-Plasmonic Nanosensor for the Determination of MMP-2 Activity Based on SERS-Fluorescence Dual-Mode Signals. *Biosens. Bioelectron.* **2022**, *212*. https://doi.org/10.1016/j.bios.2022.114389.

(43) Yin, L.; Sun, H.; Zhang, H.; He, L.; Qiu, L.; Lin, J.; Xia, H.; Zhang, Y.; Ji, S.; Shi, H.; Gao, M. Quantitatively Visualizing Tumor-Related Protease Activity in Vivo Using a Ratiometric Photoacoustic Probe. *J. Am. Chem. Soc.* **2019**, *141* (7), 3265–3273. https://doi.org/10.1021/jacs.8b13628.

(44) Li, S.-Y.; Cheng, Q.-X.; Liu, J.-K.; Nie, X.-Q.; Zhao, G.-P.; Wang, J. CRISPR-Cas12a Has Both Cis- and Trans-Cleavage Activities on Single-Stranded DNA. *Cell Res*. https://doi.org/10.1038/s41422-018.

(45) Wang, B.; Wang, R.; Wang, D.; Wu, J.; Li, J.; Wang, J.; Liu, H.; Wang, Y. Cas12aVDet: A CRISPR/Cas12a-Based Platform for Rapid and Visual Nucleic Acid Detection. *Anal. Chem.* **2019**, *91* (19), 12156–12161. https://doi.org/10.1021/acs.analchem.9b01526.

(46) Feng, W.; Newbigging, A. M.; Tao, J.; Cao, Y.; Peng, H.; Le, C.; Wu, J.; Pang, B.; Li, J.; Tyrrell, D. L.; Zhang, H.; Le, X. C. CRISPR Technology Incorporating Amplification Strategies: Molecular Assays for Nucleic Acids, Proteins, and Small Molecules. *Chem. Sci.* **2021**, *12* (13), 4683–4698. https://doi.org/10.1039/d0sc06973f.

(47) *Anaspec Home Page https://www.anaspec.com/ (accessed 2023-10-29).*

BPS Bioscence Home Page https://bpsbioscience.com/ (accessed 2023-10-29).

(48) Fang, Y.; Li, Y.; Li, Y.; He, R.; Zhang, Y.; Zhang, X.; Liu, Y.; Ju, H. In Situ Protease Secretion Visualization and Metastatic Lymph Nodes Imaging via a Cell Membrane-Anchored Upconversion Nanoprobe. *Anal. Chem.* **2021**, *93* (19), 7258–7265. https://doi.org/10.1021/acs.analchem.1c00469.

(49) Bruch, R.; Urban, G. A.; Dincer, C. CRISPR/Cas Powered Multiplexed Biosensing. *Trends Biotechnol.* **2019**, *37* (8), 791–792. https://doi.org/10.1016/j.tibtech.2019.04.005.

(50) Phan, Q. A.; Truong, L. B.; Medina-Cruz, D.; Dincer, C.; Mostafavi, E. CRISPR/Cas-Powered Nanobiosensors for Diagnostics. *Biosens. Bioelectron.* **2022**, *197*. https://doi.org/10.1016/j.bios.2021.113732.

(51) Bertucci, A.; Porchetta, A.; Del Grosso, E.; Patiño, T.; A.; Idili, A.; Ricci, F. Protein-Controlled Actuation of Dynamic Nucleic Acid Networks by Using Synthetic DNA Translators. *Angew. Chem. Int. Ed.* **2020**, *59*, 20577–20581. https://doi.org/10.1002/anie.202008553.

(52) Bucci, J.; Irmisch, P.; Del Grosso, E.; Seidel, R.; Ricci, F. Orthogonal Enzyme-Driven Timers for DNA Strand Displacement Reactions. *J. Am. Chem. Soc.* **2022**, *144* (43), 19791–19798. https://doi.org/10.1021/jacs.2c06599.

(53) Xiang, Z.; Zhao, J.; Yi, D.; Di, Z.; Li, L. Peptide Nucleic Acid (PNA)-Guided Peptide Engineering of an Aptamer Sensor for Protease-Triggered Molecular Imaging. *Angew. Chem. Int. Ed.* **2021**, *60* (42), 22659–22663. https://doi.org/10.1002/anie.202106639.

(54) Watson, E. E.; Angerani, S.; Sabale, P. M.; Winssinger, N. Biosupramolecular Systems: Integrating Cues into Responses. *J. Am. Chem. Soc.* **2021**, *143* (12), 4467–4482. https://doi.org/10.1021/jacs.0c12970.

Supporting Information

Synthetic Protein-to-DNA Input Exchange for Protease Activity Detection Using CRISPR-Cas12a

*Luca Capelli,[a] Federica Pedrini, [a] Andrea Di Pede, [b] Neda Bagheri, [b] Simone Fortunati, [a] Marco Giannetto, [a] Monica Mattarozzi, [a] Roberto Corradini, [a] Alessandro Porchetta, [b] Alessandro Bertucci[a]**

[a] Department of Chemistry, Life Sciences and Environmental Sustainability, University of Parma, Parco Area Delle Scienze 17/A, 43124, Parma, Italy

[b] Department of Chemistry, University of Rome Tor Vergata, Via della Ricerca Scientifica 1, 00133 Rome, Italy

Supporting Information

1. Materials and Methods

2. Supporting Figures

3. References

1. MATERIALS AND METHODS

1.1 Chemicals

Tris(hydroxymethyl)-aminomethane was purchased from Tokyo Chemical Industry (Tokyo, Japan). Sodium chloride was purchased from VWR chemicals (Leuven, Belgium). Calcium chloride, Acetic anhydride, Dimethyl sulfoxide, *N,N*-Dimethylformamide (DMF) for peptide synthesis and *N*-Methyl-2-pyrrolidone were purchased from Carlo Erba (Milan, Italy). DBCO-NHS was purchased from BroadPharm (San Diego, CA, USA). Amine-terminated magnetic particles (1µM in size), Azidoacetic acid, Diethyl ether, Dichloromethane, m-Cresol and Acetonitrile were purchased from Sigma Aldrich (Merck KGaA, Darmstadt, Germany). *N,N*-Diisopropylethylamine and Imidazole were purchased from Alfa Aesar (Ward Hill, MA,USA). Hydroxylamine hydrochloride was purchased from VWR (Radnor, PA, USA). Piperidine, *O-(1H*-Benzotriazol-1-yl*)-N,N,N′,N′*-tetramethyluronium hexafluorophosphate (HBTU) and Trifluoroacetic acid (TFA) were purchased from abcr GmbH (Karlsrhue, Germany). EnGen Lba Casa12a (Cpf1) was purchased from new England BioLabs (Ipswich, MA, USA).

1.2 Recombinant human proteases

Recombinant human MMP-2 was purchased from BIO RAD (Hercules, CA, USA). Human MMP-12 HME protein (catalytic domain), human MMP-1 protein (His Tag), and human MMP-9 CLG4B protein (His Tag) were purchased from Sino Biological (Beijing, China).

1.3 Oligonucleotides

All the RNA and DNA sequences used in this work were purchased from Metabion international AG (Planegg, Germany). The specific sequences are reported below:

Hairpin DNA reporter

5’ - (6-FAM) - CTCTCATTTTTTTTTAGAGAG - (BHQ1) - 3’

6- FAM is 6-Carboxyfluorescein

BHQ1 is Black Hole Quencher 1

crRNA

5’ – UAAUUUCUACUAAGUGUAGAUUUUAGUCUACACAUGGCUAAAUCU – 3’

CRISPR-Cas12a target DNA (DNA Activator)

5’ – *AGATTTAGCCATGTGTAGACTAAA*TTTTTTAGTTCTAAGC - 3’

Highlighted in italic is the domain complementary to the RNA sequence in the Cas12a/crRNA complex.

Underlined is the domain complementary to the PNA sequence in the peptide-PNA translator.

1.4 Synthesis of the Peptide-PNA chemical translator

The synthesis of the peptide-PNA conjugates utilized as chemical translators was performed with standard manual Fmoc-based solid-phase synthesis using HBTU/DIPEA as coupling mixture, and commercially available Fmoc-AA-OH monomers (Sigma Aldrich, Merck KGaA, Darmstadt, Germany) and Fmoc-PNA-OH monomers (Biosearch Technologies, Bellshill, Scotland), following

an established protocol.[1] Rinkamide-ChemMatrix resin was first loaded with Fmoc-Lys$_{(Dde)}$-OH as the first monomer (0.13 mmol/g). Two versions of peptide-PNA translators that differ for the presence of a fluorescent tag were prepared. Both the translators have the same peptide-PNA sequences (reported below), with an azide group at the N-end. The azide group was introduced by reacting the translator with preactivated azidoacetic acid using HBTU/DIPEA as an activating mixture. Prior to cleavage from the resin, the Dde (2-Acetyldimedone) protecting group on the side chain of the lysine residue was removed with a solution of *N*-Methyl-2-pyrrolidone, hydroxylamine and imidazole in DMF. In the case of the peptide-PNA translator labelled with a fluorescent tag, the side chain of the lysine was used as anchor point for a TAMRA molecule, which was introduced by reacting preactivated (through HBTU/DIPEA mixture) 5(6)-Carboxy-tetramethylrhodamine with the amino group on the translator. Cleavage from resin was performed with a solution of 10% m-cresol in trifluoroacetic acid (TFA).

Peptide-PNA translator
5' - N3 – O* - *GPLGVRG* - GCTTAGAACT – K - NH_2 – 3'

Peptide-PNA translator labelled with a fluorescent tag
5' - N3 – O* - *GPLGVRG* - GCTTAGAACT – K – NH_2 – 3'
|
TAMRA**

N3 azide
* 2-[2-(Fmoc-amino)ethoxy]ethoxyacetic acid (AEEA) (Biosearch Technologies, Bellshill, Scotland
** 5(6)-Carboxy-tetramethylrhodamine (Novabiochem, Merck KGaA, Darmstadt, Germany)

Highlighted in italic is the sequence of the peptide unit.

The purification of the above peptide-PNA conjugates was performed by RP-HPLC (Agilent 1260 Infinity) with UV detection at λ 260 nm using a semi-preparative C_{18} column (5 µm, 250×10 mm, Jupiter Phenomenex, 300 Å), eluting with H_2O containing 0.1 % TFA (eluent A) and CH_3CN containing 0.1 % TFA (eluent B); elution gradient: from 100 % A to 50 % B over 30 min, flow rate: 4 mL min^{-1}.

The purity and identity of the purified peptide-PNA conjugates were determined by HPLC–ESI/MS (Dionex Ultimate 3000 equipped with linear ion trap detector) using a Phenomenex Gemini C_{18} column: 100×4.6 mm, 3 µm.

1.5 Analysis of MMP2-mediated proteolytic cleavage of the peptide-PNA translator

A solution of peptide-PNA chemical translator (0.5 µM) in TRIS containing $CaCl_2$ 1 mM was incubated with MMP2 at a 1:0.1 ratio for 24 hours at 37° C. The analyses were conducted using a Dionex Ultimate 3000 High-Performance Liquid Chromatography (HPLC) system (Thermo Scientific) coupled to an Orbitrap LTQ XL mass spectrometer (Thermo Scientific). Chromatographic separation was achieved using a Kinetex C18 column (Phenomenex, 50 x 2.1 mm, 2.6 µm, 100 Å). The instrument operated via gradient elution with a mobile phase composed of Phase A (0.1% formic acid v/v in water) and Phase B (0.1% formic acid v/v in acetonitrile); elution gradient: from 99 % A to 95 % B over 40 min. The mobile phase flow rate and injection volume were set at 200 µL/min and 5 µL, respectively, with an acquisition delay of 3.50 minutes.

1.6 Functionalization of magnetic beads with the peptide-PNA translator

Aminated magnetic beads (0.1 mg/mL) were initially washed with pure DMSO, then resuspended in a 2.5 mM solution of DBCO-NHS in DMSO added with DIPEA and incubated for 2 h at 25 °C under constant shaking (1500 rpm). After that, the beads were washed with DMSO to remove unreacted DBCO-NHS and incubated with a fresh solution of azide-modified peptide-PNA translator in TRIS buffer (0.1 mg/mL) for 3.5 h at 37 °C. Eventually, the beads were washed thrice with distilled water.

To optimize the conditions for the SPAAC reaction, the use of different solvents was explored. These were aqueous TRIS buffer, water, and a water/DMSO 1:1 mixture, as reported in Table S1. The fluorescent version of the translator labeled with tetramethylrhodamine (TAMRA) was used in these experiments. Fluorescence spectroscopy measurements of the peptide-PNA solution before and after incubation with the DBCO-modified magnetic beads were used to calculate the quantity of translator immobilized on the beads, expressed as loading (nmol/mg) and loading % w:w.

	TRIS buffer	H_2O	H_2O/DMSO (1:1)
Moles of translator attached to 0.1 mg magnetic beads	$1{,}04 \cdot 10^{-9}$	$8 \cdot 10^{-10}$	$3{,}47 \cdot 10^{-10}$
Loading (nmol/mg)	10,4	8	3,47
Loading % w:w.	4,11	3,19	1,4

Table S1. Comparison of the functionalization efficiency for DBCO-functionalized magnetic beads (0.1 mg/mL) incubated with fluorescent azide-presenting peptide-PNA translator (1 mg/mL) using different reaction solvents.

1.7 Characterization of the functionalization steps

ATR- FT-IR measurements were conducted using a Thermo Scientific Nicolet 5PCFT-IR-ATR spectrophotometer. Zeta Potential (Malvern Zetasizer Nano ZSP) measurements were performed in PBS buffer pH 7.4. Fluorescence measurements were conducted using a Horiba Jobin-Yvon Fluoromax-3 spectrophotometer. These were performed, using quartz cuvettes of reduced volume (100 µL). Working wavelengths were set to λ_{exc} = 550 nm and λ_{em} = 555-700 nm to monitor the fluorescence emission of TAMRA, and all measurements were performed at room temperature. Two-photon microscopy images of magnetic beads functionalized with the TAMRA-labeled peptide-PNA translator were acquired using a vertical Nikon A1R MP+ two-photon microscope equipped with a femtosecond pulsed laser from Coherent Chameleon Discovery.

1.8 Loading curve

DBCO-functionalized magnetic beads (0.1 mg/mL) were incubated with solutions of the fluorescent peptide-PNA of different concentrations (0.01, 0.1, 1, 5, 10, 24 µM), following the protocol described above. Fluorescence spectroscopy measurements of the peptide-PNA solution before and after incubation with the DBCO-modified magnetic beads were used to calculate the quantity of translator covalently immobilized on the bead surface. The emission intensity of the TAMRA fluorophore conjugated to the peptide-PNA translator was collected in solution at λ_{Em} = 584 nm (λ_{Ex} = 550 nm) before and after the translator immobilization on the magnetic beads. The fluorescence intensity

reduction expressed in percentage was used to estimate the number of moles attached to the magnetic beads. The measurements were replicated three times, and the value obtained is reported as the mean value ± standard deviation (Figure S4).

1.9 Kinetic analysis of MMP2-mediated proteolytic cleavage

Magnetic beads functionalized with the fluorescent peptide-PNA translator were incubated with MMP2 (100 nM) for 1, 2, 4 and 8 h, respectively. The supernatant was then collected and analyzed by means of fluorescence spectroscopy as described above.

1.10 Specificity assay

MMP1, MMP9 and MMP12 (100 nM solution in TRIS buffer 1 M containing $CaCl_2$ 1 mM) were respectively incubated with magnetic beads functionalized with the fluorescent peptide-PNA Translator (1 mg/mL) for 2 h at 37°C. The supernatant was then collected and analyzed by means of fluorescence spectroscopy as described above.

1.11 Quantitative fluorescence-based assay

Magnetic beads functionalized with the fluorescent peptide-PNA translator (1 mg/mL) were incubated with varying concentrations of MMP2 in the range 0.03 - 10 nM (2h at 37°C). The supernatant was then collected and analyzed by means of fluorescence spectroscopy as described above. The limit of detection (LOD) was determined according to Eurachem guidelines (https://www.eurachem.org).

1.12 CRISPR-Cas12a-assisted activity-based assays

Magnetic beads covalently conjugated with peptide-PNA translators were prepared as described above (1 mg/ml) and subsequently incubated with a 10 µM solution of the ssDNA activator sequence (2h at 37°C), then washed twice with distilled water. The obtained PNA:DNA-modified beads were incubated with varying concentrations of MMP2 in the range 0.3 - 300 pM. The resulting supenatant was collected and used for subsuquent analysis. The LbCas12a-mediated cleavage assays were carried out adding 7.5 µl of Cas12a/cRNA complex (200 nM, in a buffer consisting of 10 mM Tris-HCl (pH 7.9), 50 mM NaCl, and 100 mM $MgCl_2$) previously incubated (30 min at 37°C) to 67.5 µl of supernatant solution containing the Hairpin DNA reporter (final concentration 100 nM). Kinetics were followed for 2h at 37 °C by utilizing a microplate reader Tecan Infinite 200 pro using top reading mode with black, flat bottom non-binding 96-well plates. The fluorescence intensity values were expressed in terms of signal gain % (calculated with the following formula: signal gain % = (Fluorescence Signal – Background) / Background * 100, where the Background is the signal observed when conducting the assay in the absence of MMP2) as a function of different MMP2 concentrations and analyzed using a linear regression model in PRISM (GraphPad).

2. SUPPORTING FIGURES

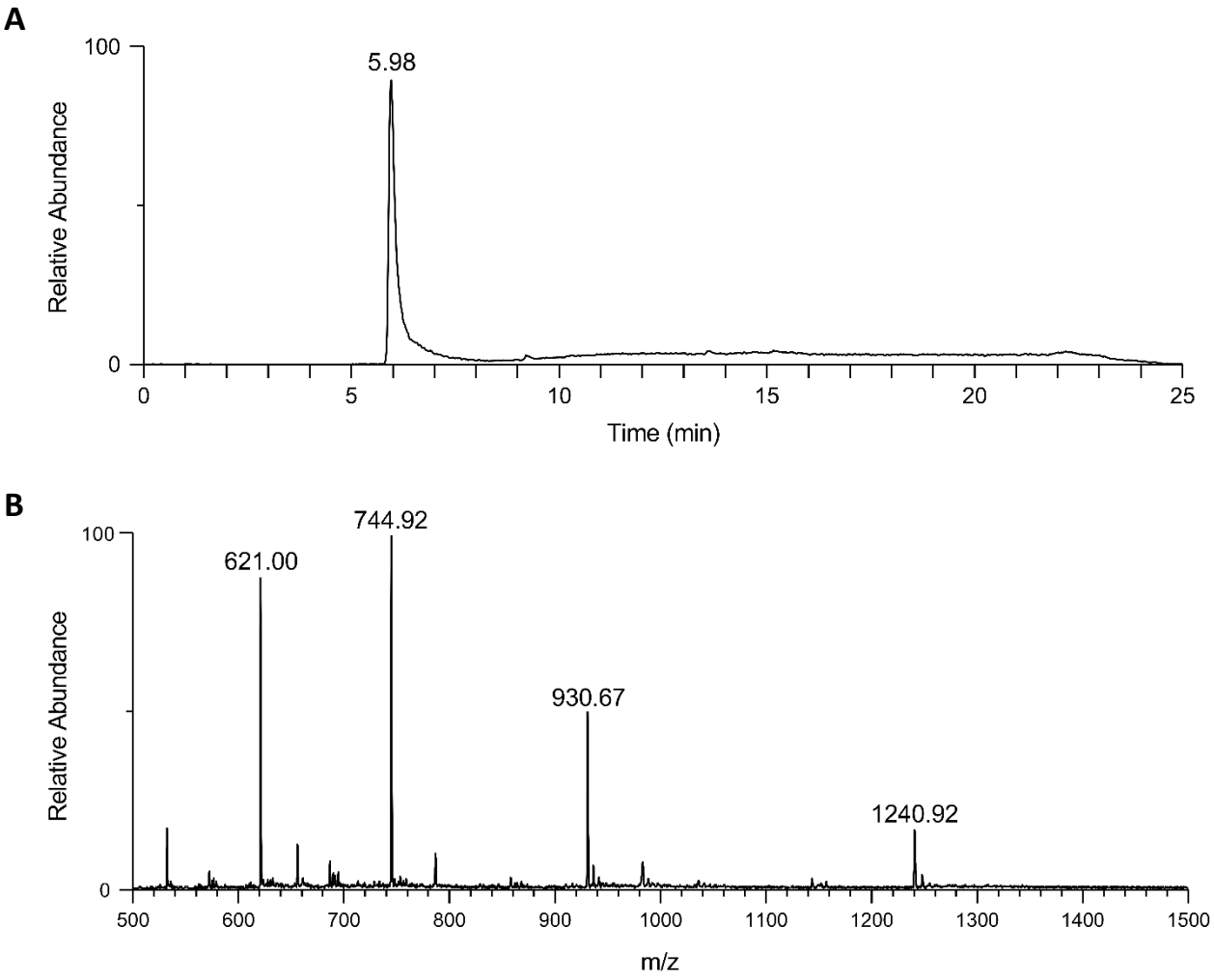

Figure S1. A) UPLC–ESI/MS (Waters Acquity equipped with SQ detector) chromatogram of the PNA-peptide translator; B) Mass spectrum of the chromatographic peak at time = 5.98 min, corresponding to the peptide-PNA translator, *m/z* found (calculated) = 621.00 (620.95) $[M+6H]^{6+}$, 744.92 (744.96) $[M+5H]^{5+}$, 930.67 (930.95) $[M+4H]^{4+}$, 1240.92 (1240.93) $[M+3H]^{3+}$.

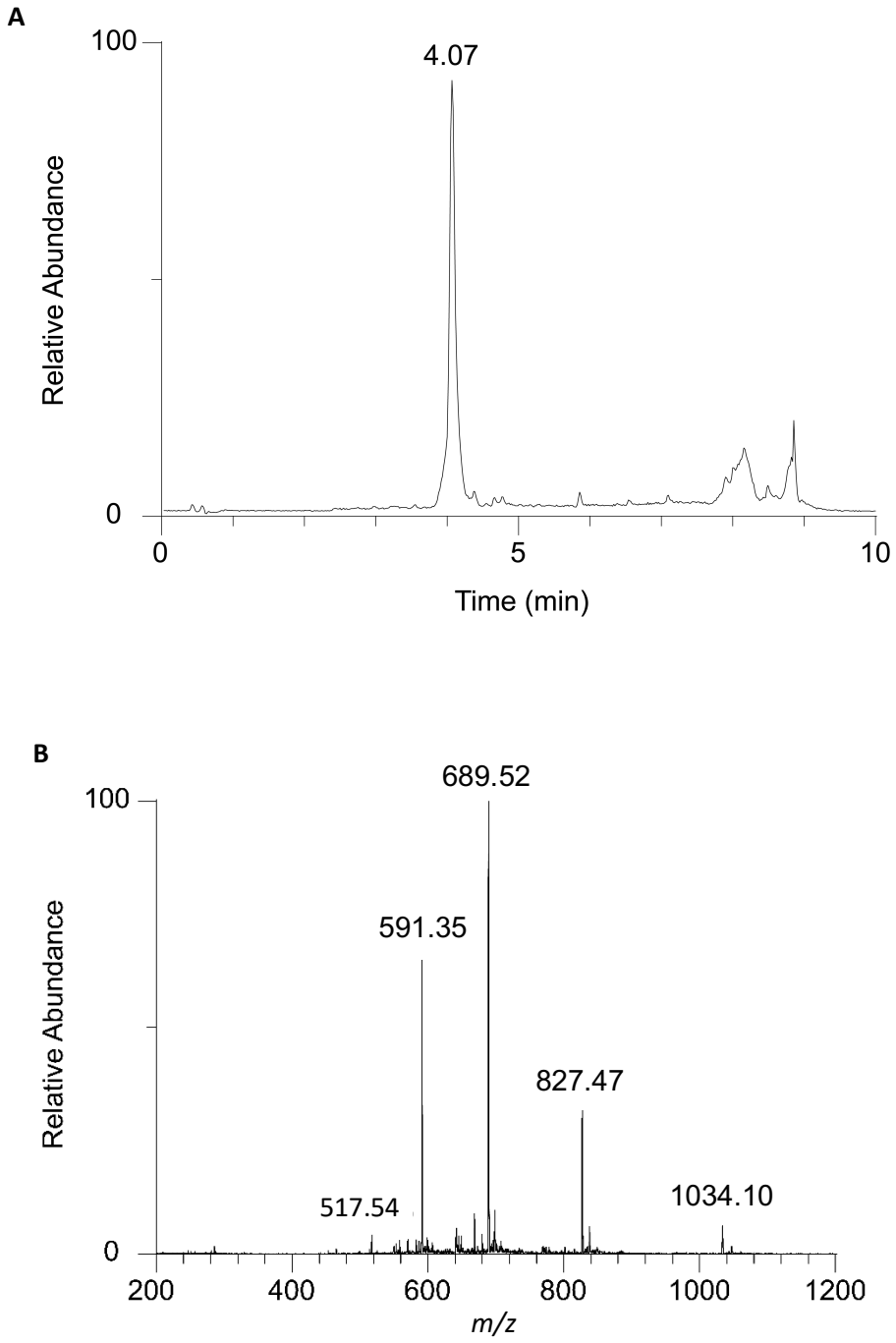

Figure S2. A) UPLC–ESI/MS (Waters Acquity equipped with SQ detector) chromatogram of the PNA-peptide translator labelled with fluorescence tag; B) Mass spectrum of the chromatographic peak at time = 4.07 min, corresponding to the peptide-PNA translator, *m/z* found (calculated) = 517.54 (517.53) $[M+8H]^{8+}$, 591.35 (591.32) $[M+7H]^{7+}$, 689.52 (689.71) $[M+6H]^{6+}$, 827.47 (827.45) $[M+5H]^{5+}$, 1034.10 (1034.06) $[M+4H]^{4+}$.

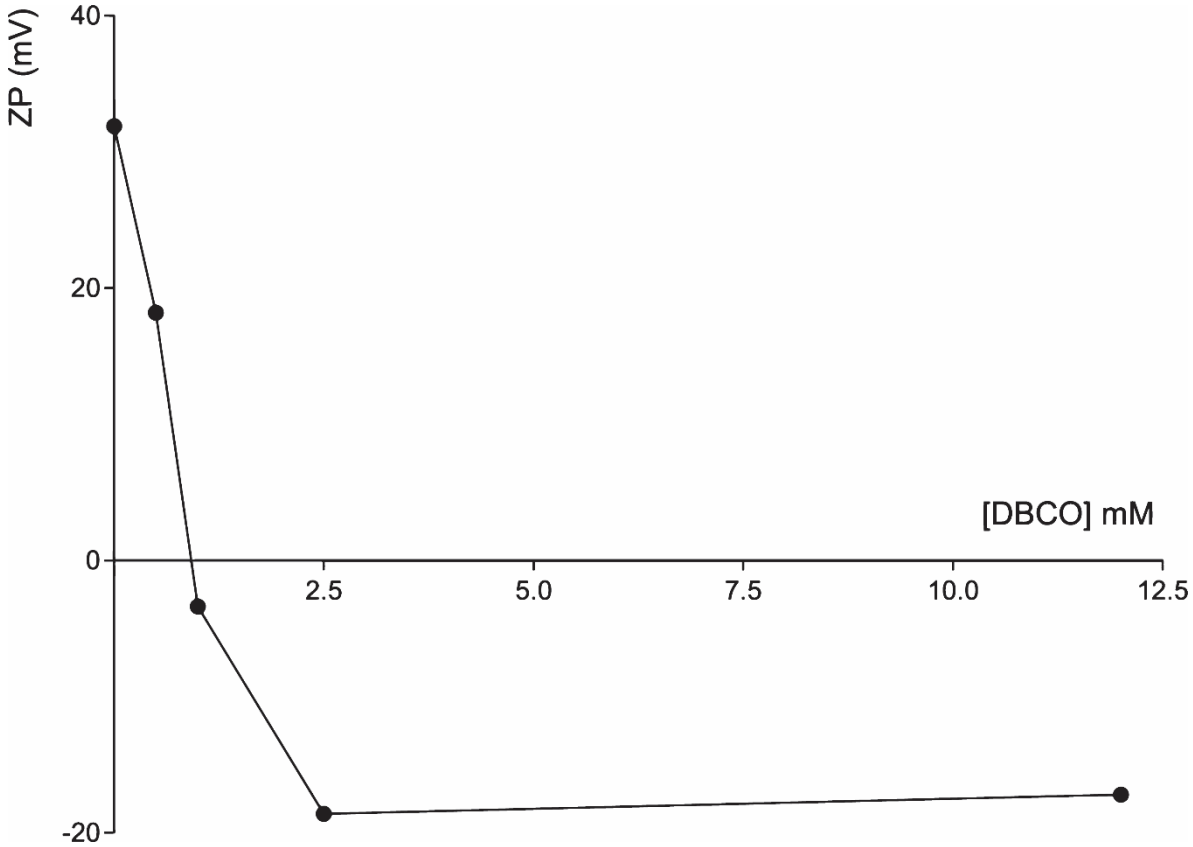

Figure S3. Zeta potential values for samples of magnetic microbeads incubated with different concentrations of DBCO-NHS in DMSO (0 mM; 0.5 nM; 1 mM; 2.5 mM; 12mM).

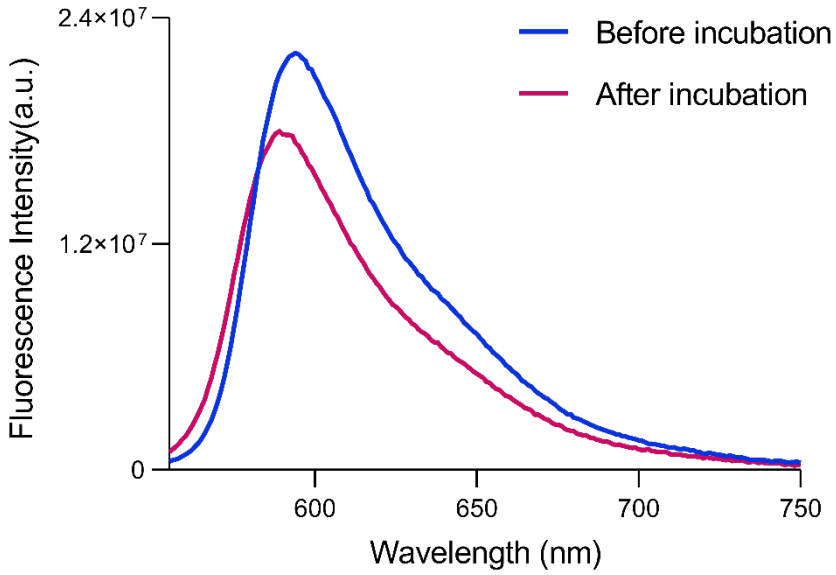

Figure S4. Fluorescence emission spectra (λ_{ex} = 550 nm) of a solution of TAMRA-labeled peptide-PNA translator in TRIS buffer (24 μM) before (blue line) and after (purple line) incubation with DBCO-functionalized magnetic beads (0.1 mg).

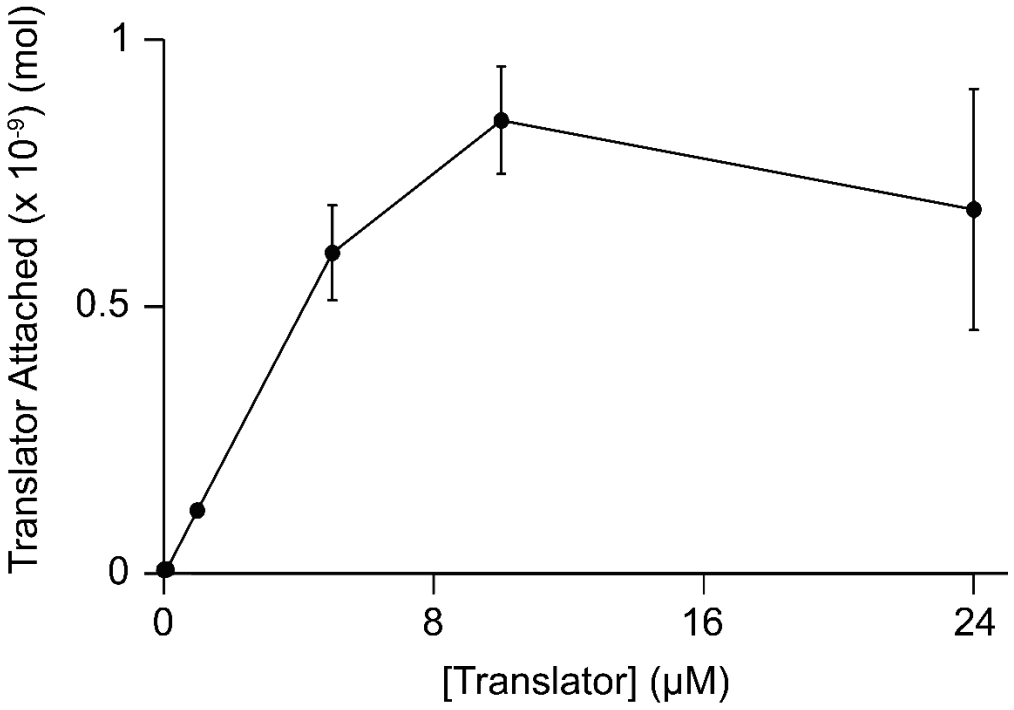

Figure S5. Moles of fluorescent peptide-PNA translator attached to the surface of magnetic beads (0.1 mg) incubated with different concentrations of translator in a range of 1-24 μM.

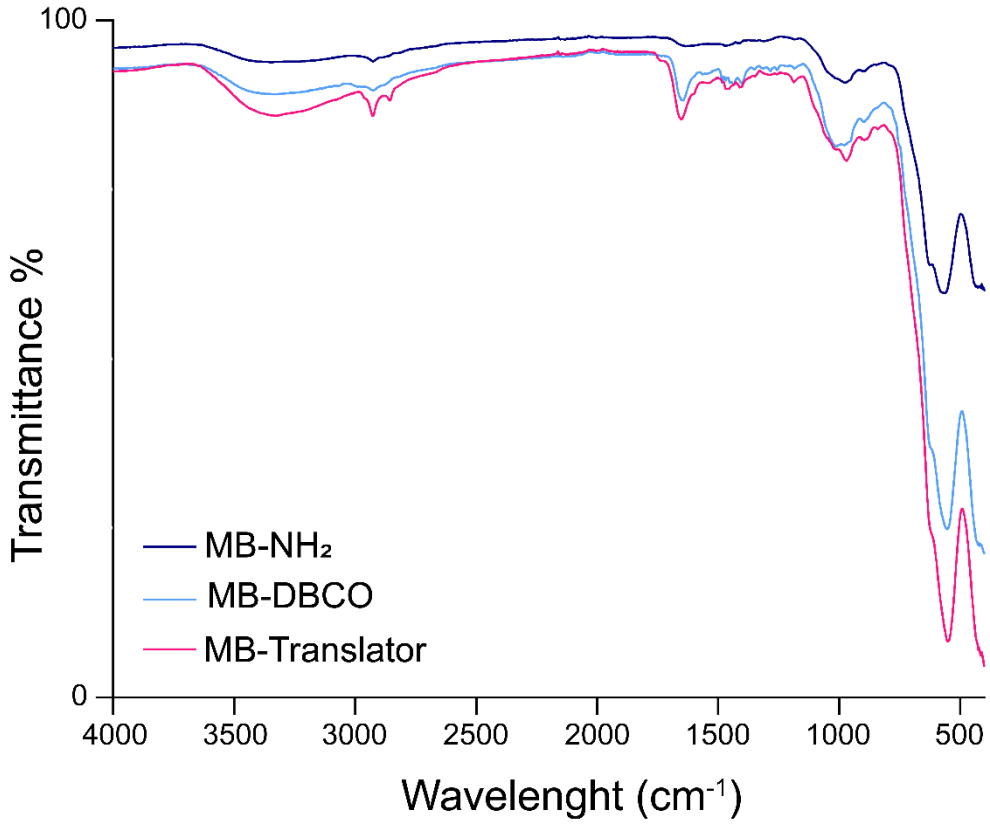

Figure S6. ATR-FT-IR spectra of aminated magnetic beads (MBs-NH_2, blue line), magnetic beads after incubation and functionalization with NHS-DBCO (MBs-DBCO, light blue line), magnetic beads after functionalization with the peptide-PNA translator (MBs-translator, purple line).

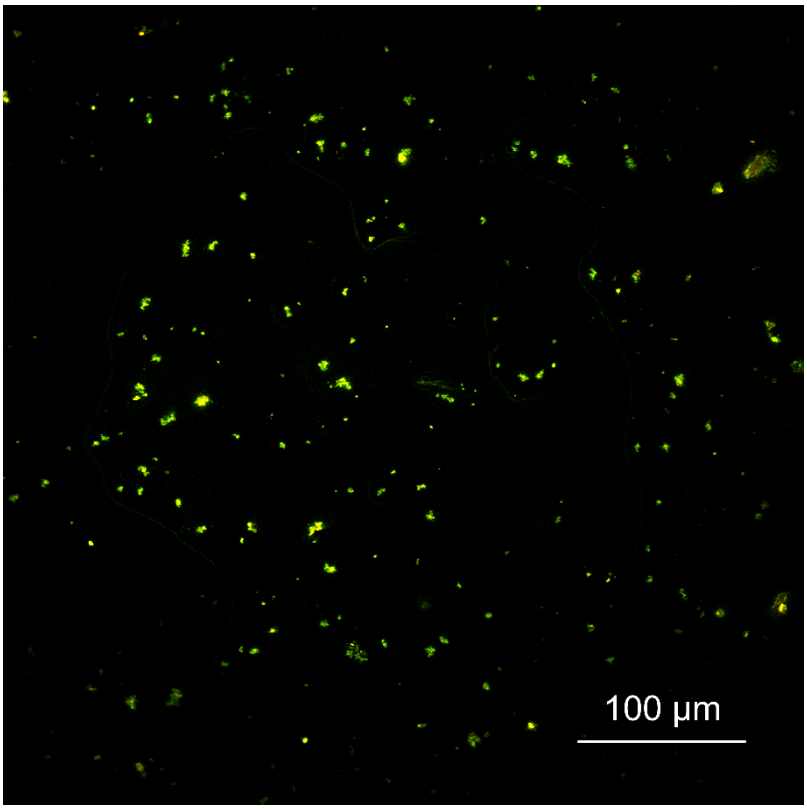

Figure S7. Two-photon microscopy image of magnetic beads functionalized with the fluorescent TAMRA-labeled peptide-PNA translator.

3. References

[1] A. Manicardi, A. Calabretta, M. Bencivenni, T. Tedeschi, S. Sforza, R. Corradini, R. Marchelli, Chirality 2010, 22, E161.